European Radiology (2019) 29:5129–5138
https://doi.org/10.1007/s00330-019-06053-7

MAGNETIC RESONANCE

Diagnostic performance of MRI for detecting intraplaque hemorrhage in the carotid arteries: a meta-analysis

Tao Zhou[1] · Shouqiang Jia[1] · Xiu Wang[2] · Bin Wang[3] · Zhiguo Wang[4] · Ting Wu[1] · Ying Li[1] · Ying Chen[1] · Chenxiao Yang[1] · Qingguo Li[1] · Zhen Yang[4] · Min Li[4] · Gang Sun[4]

Received: 11 October 2018 / Revised: 11 January 2019 / Accepted: 30 January 2019 / Published online: 7 March 2019

Abstract

Objectives To investigate the diagnostic performance of MRI in diagnosing carotid atherosclerotic intraplaque hemorrhage (IPH) and to provide a clinical guide for MRI application.

Methods We searched MEDLINE, Embase, and Cochrane library from the earliest available date of indexing through November 30, 2017. All investigators screened and selected studies comparing the use of MRI with histology. The accuracy to diagnose pathological IPH was expressed by sensitivity, specificity, negative likelihood ratios (LRs), positive LRs, and the area under summary receiver-operating characteristic (SROC) curve. We calculated the post-test probability to assess the clinical utility of MRI.

Results We analyzed 696 patients from 20 articles. The sensitivity and specificity were 87% (95% CI, 81–91%) and 92% (95% CI, 87–95%), respectively. The positive and negative LRs were 10.27 (95% CI, 6.76–15.59) and 0.15 (95% CI, 0.10–0.21), respectively. The area under SROC curve was 0.95 (95% CI, 0.93–0.97). MRI was accurate in confirming or in ruling out disease over a wide range of pre-test probabilities of IPH: MRI could increase the post-test probability to > 80% in patients with a pre-test probability > 27% and could decrease the post-test probability to < 20% in patients with a pre-test probability < 64%.

Conclusion Non-invasive MRI has excellent specificity and good sensitivity for diagnosing IPH. MRI is a tool for confirming or ruling out carotid atherosclerotic IPH.

Key Points

- *Non-invasive MRI has excellent performance for diagnosing IPH, which is a component of vulnerable plaque.*
- *The high accuracy of MRI for IPH helps clinicians analyze the prognosis of clinical events and plan personalized treatment.*

Keywords Carotid artery plaque · Hemorrhage · Stroke · Magnetic resonance imaging

Tao Zhou and Shouqiang Jia contributed equally to this work and are first authors.

Electronic supplementary material The online version of this article (https://doi.org/10.1007/s00330-019-06053-7) contains supplementary material, which is available to authorized users.

✉ Min Li
liminyingxiang@163.com

✉ Gang Sun
Gangsunvip@163.com

[1] Department of Radiology, Laiwu Affiliated Hospital of Taishan Medical University, Laiwu, China

[2] Department of ICU, Laiwu Affiliated Hospital of Taishan Medical University, Laiwu, China

[3] Department of Health Care, Shandong University Affiliated Jinan Center Hospital, Jinan, China

[4] Department of Medical Imaging, 960 Hospital of PLA, No. 25, Shifan Road, Jinan 250031, Shandong Province, China

Abbreviations

AUROC	Area under receiver of operating characteristic
CE	Contrast enhanced
CI	Confidence interval
DTI	Direct thrombus imaging
FFE	Fast field echo
FSE	Fast-spin echo
GRE	Gradient recalled echo
IPH	Intraplaque hemorrhage
LR	Likelihood ratio
MRA	MR angiography
MRI	Magnetic resonance imaging
PDWI	Proton density weighted imaging
QUADAS	Quality Assessment of Diagnostic Accuracy Studies
RAGE	Rapid acquisition gradient echo
SE	Spin echo
SROC	Summary receiver-operating characteristic

T1WI	T1-weighted imaging
T2WI	T2-weighted imaging
TFE	Turbo field echo
TOF	Time of flight
TSE	Turbo spin echo

Introduction

Stroke related to atherosclerosis is one of the most serious diseases threatening human beings' health [1, 2]. The severity of carotid atherosclerotic stenosis was long thought to be the risk factor for stroke, and the level of carotid stenosis served as a principal criterion in deciding whether to use surgical treatment or drug therapy to treat carotid atherosclerotic disease [3, 4]. Vulnerable carotid plaque, independent of the stenosis severity, is also an important risk factor [5, 6]. Vulnerable carotid plaque is defined as unstable lesions connected with an increased risk of rupture and thromboembolic events [7, 8]. The main components of vulnerable plaque are intraplaque hemorrhage (IPH), lipid-rich necrotic cores, ulceration, or thin fibrous caps [7, 8]. Compared with other specific histopathologic features, IPH plays a more important role in the progression of plaque [9]. According to the American Heart Association histologic classification of atherosclerotic plaques, IPH is a key component of type VI plaque, known as complicated plaque and exposing to serious complications [10, 11].

Tools for evaluation of IPH should be non-invasive and easily accessible in daily clinical practice. Different non-invasive imaging methods have the potential to recognize carotid vulnerable plaques in vivo [12–17]. However, carotid ultrasonography, contrast-enhanced ultrasound, shear wave elastography, and multidetector-row computed tomography (CT) cannot accurately diagnose IPH or provide detailed information about a vulnerable plaque [12–17]. Magnetic resonance imaging (MRI) has an excellent capability for distinguishing IPH [18–20]. However, published studies have shown variation in the diagnostic performance, probably explained by the selection and number of patients examined in single centers. Finally, it is uncertain whether MRI has the ability to confirm IPH, or exclude IPH, or both confirm and exclude IPH.

This is not only important for the prognosis of clinical events but also for guiding personalized surgical or pharmacological treatment. The objective of our meta-analysis was to systematically evaluate the accuracy of MRI in diagnosing carotid IPH, with histology as the gold standard, and to analyze the diagnostic role of MRI for confirming or excluding the presence of IPH.

Methods

Data sources and searches

This diagnostic meta-analysis adhered to the statement of the Preferred Reporting Items for Systematic Reviews and Meta-Analyses. We searched MEDLINE, Embase, and Cochrane library from the earliest available date of indexing through November 30, 2017, without language restrictions.

Selection criteria

Our search strategy is shown in the supplementary material. We selected articles by first using two investigators to examine their titles and abstracts. The pre-specified inclusion and exclusion criterions are listed in the supplementary material.

Data extraction and quality assessment

The recording data for each eligible study are listed in the supplementary material. Two independent investigators evaluated the study quality with the Quality Assessment of Diagnostic Accuracy Studies (QUADAS) tool [21].

Statistical analysis

We used Cohen's kappa test to evaluate the inter-observer agreement. To avoid publication bias, we constructed an effective sample-size funnel plot versus the log diagnostic odds ratio and carried out the regression test of asymmetry [22]. As we anticipated that the heterogeneity would be significant, we used an exact binomial rendition of the bivariate mixed-effects regression model with test type as a random-effects covariate, which accounted heterogeneity among the original studies, to synthesize the summary operating sensitivity, specificity, and the positive and negative likelihood ratios (LRs) [23, 24]. Based on a random-effects analysis, we evaluated the heterogeneity by calculating the Cochran Q statistic and I^2 statistic [25]. We also applied a meta-regression to analyze the predictors that influenced the heterogeneity [23].

Based on the parameters estimated by the bivariate model for the logit transforms of sensitivity and specificity between the studies, we constructed a hierarchical summary receiver-operating characteristic (SROC) curve, the area under which represented as a global performance of MRI. The values for the area under receiver of operating characteristic (AUROC) were defined as high (0.9–1), moderate (0.7–0.9), or low (0.5–0.7). According to Bayes' theorem, we calculated the post-test probability to assess the clinical utility of MRI [26]. Given a pre-test probability of vulnerable IPH and the work of a special test by the aid of its LRs, we can evaluate the post-test probability of IPH after conducting this test. Using this

approach, one can confirm (if the post-test probability goes beyond 80%) or exclude (if the post-test probability drops below 20%) the carotid atherosclerotic IPH.

We analyzed the data and constructed the graphs with Stata, version 12 (StataCorp) and applied SPSS, version 16.0 (SPSS), to calculate the kappa statistics.

Results

We found 1843 articles from MEDLINE, 3176 from Embase, and 124 from Cochrane library. After screening by title and abstract, we retrieved 331 full articles. Of these articles, 20 met our inclusion criteria. A flow chart describing our research and selection process is presented in Fig. 1.

Study characteristics

Table 1 summarizes the details of the articles. We included the data of 696 patients from the 20 studies.

The QUADAS assessment for the 20 studies is summarized in supplementary Table 1. We evaluated the methodological quality according to the QUADAS tool. The inter-observer consistency was good ($K = 0.93$).

Summary of the diagnostic performance measures

The publication bias was not significant ($p = 0.133$), which is shown in supplementary Fig. 1.

The summary sensitivity and specificity were 87% (95% CI, 81–91%) and 92% (95% CI, 87–95%), respectively. We found a significant heterogeneity for both sensitivity and

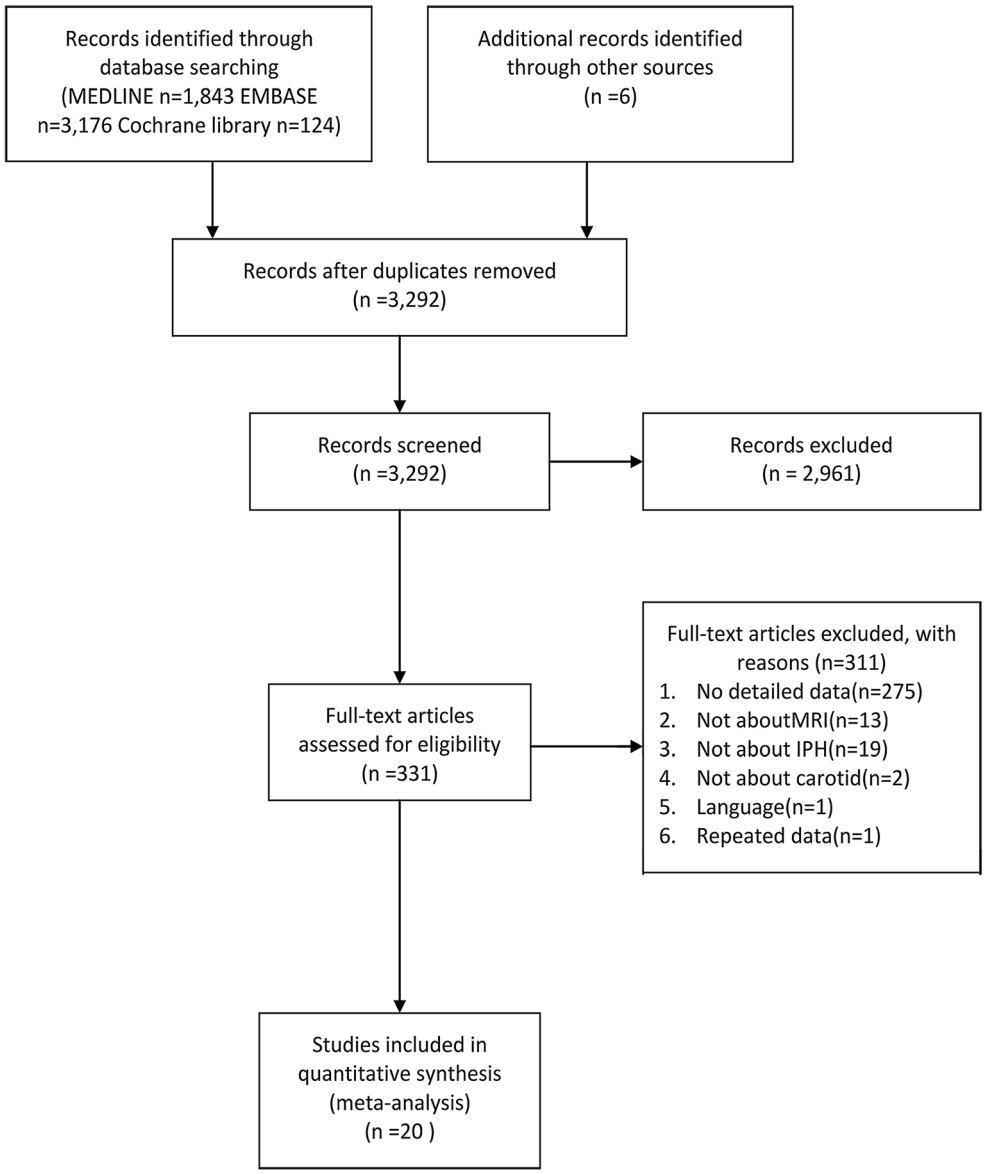

Fig. 1 The protocol of evidence search and selection. Twenty studies were ultimately identified

Table 1 Characteristics of included studies

First author	Year	No. of patients	Age	Male/all	Scanner brand	Magnet strength	MRI sequence	Prevalence			
								Smoking	Hypertension	Hypercholesterolemia	Diabetes
Chai, J. T. et al [19]	2016	26	67.5	–	Siemens	3.0 T	2D TOF, T2WI maps	0.42	0.88	–	0.3
Narumi, S. et al [20]	2015	31	70.8	0.9	GE	1.5 T	3D-T1WI (FSE)	–	0.78	0.75	0.31
Lukanova, D. V. et al [27]	2015	25	66	0.75	Siemens	1.5 T	T1WI (TSE), T2WI, PDWI, CE-MRA	–	–	–	–
Millon, A. et al [28]	2013	79	70	0.71	Philips	3.0 T	T1WI (TSE), TOF, PDWI	0.44	0.76	0.59	0.31
Narumi, S. et al [29]	2013	30	69.5	1.00	Hitachi	1.5 T	T1WI (SE)	–	0.95	0.55	0.33
Qiao, Y. et al [30]	2011	15	–	–	Philips	3.0 T	CE-MRA (3D FFE sequence)	–	–	–	–
Ota, H. et al [31]	2010	20	67.7	0.80	GE/Philips	3.0 T	T1w 3D magnetization-prepared RAGE	0.55	0.7	0.8	0.25
Yim, Y. J. et al [32]	2008	135	62	0.63	GE	1.5 T	T1WI (FSE), 3D TOF, T2WI (FSE)	–	–	–	–
Watanabe, Y. et al [33]	2008	54	70	0.83	Philips	1.5 T	T1WI (TSE), 3D TOF, T2WI (TSE)	–	–	–	–
Bitar, R. et al [34]	2008	11	74.6	0.91	GE	1.5 T	3D-T1WI (spoiled GRE)	–	–	–	–
Esposito, L. et al [35]	2007	21	74.9	0.66	Siemens	1.5 T	T1WI (FSE), 3D TOF, T2WI, PDWI	0.62	0.85	0.55	0.31
Puppini, G. et al [36]	2007	15	72.5	0.68	Siemens	1.5 T	T1WI (TSE), 3D TOF, T2WI, PDWI	–	–	–	–
Honda, M. et al [37]	2006	17	68.6	0.82	GE	1.5 T	2D TOF	–	–	–	–
Clarke, S. E. et al [38]	2006	12	–	–	GE	1.5 T	T1WI (FSE), PDWI, DWI	–	–	–	–
Saam, T. et al [39]	2005	31	68	0.95	GE	1.5 T	T1WI (FSE), 3D TOF, T2WI, PDWI	–	–	–	–
Kampschulte, A. et al [40]	2004	24	–	–	GE	1.5 T	T1WI (FSE), TOF, T2WI, PDWI	–	–	–	–
Chu, B. et al [41]	2004	24	68.5	0.78	GE	1.5 T	T1WI (FSE), TOF, T2WI, PDWI	–	–	–	–
Cappendijk, V. C. et al [42]	2004	11	–	–	Philips	1.5 T	T1WI (TFE)	–	–	–	–
Moody, A. R. et al [43]	2003	63	69	0.52	Siemens	1.5 T	MRDTI (T1WI magnetization-prepared 3D GRE)	–	–	–	–
Cai, J. M. et al [44]	2002	52	–	–	GE	1.5 T	T1WI (FSE), 3D TOF, T2WI, PDWI	–	–	–	–

T1WI T1-weighted imaging, *T2WI* T2-weighted imaging, *PDWI* proton density–weighted imaging, *TOF* time of flight, *CE* contrast enhanced, *MRA* MR angiography, *FFE* fast field echo, *TSE* turbo spin echo, *FSE* fast-spin echo, *TFE* turbo field echo, *SE* spin echo, *DTI* direct thrombus imaging, *magnetization-prepared RAGE* magnetization-prepared rapid acquisition gradient echo, *GRE* gradient recalled echo

specificity ($I^2 = 84.18$, $p < 0.001$ and $I^2 = 75.97$, $p < 0.001$), which is shown in Fig. 2.

The SROC curve that summarizes the operating points for sensitivity and specificity reveals the high diagnostic performance of MRI in diagnosing IPH, with an area under the curve of 0.95 (95% CI, 0.93–0.97; Fig. 3).

The positive and negative LRs were 10.27 (95% CI, 6.76–15.59) and 0.15 (95% CI, 0.10–0.21), respectively (Fig. 2). We calculated the post-test probabilities to determine the implications of MRI for diagnosing IPH. The plot shows high predictive values of MRI in confirming or ruling out the disease over a wide range of pre-test probabilities of IPH: MRI could increase the post-test probability to > 80% in patients with a pre-test probability > 27% and could decrease the post-test probability to < 20% in patients with a pre-test probability < 64% (Fig. 4).

The meta-regression demonstrated that the magnetic field strength, the sequences of MRI, the mean patient age, and the percentage of male participants were significant predictors of heterogeneity ($p = 0.01$, $p = 0.04$, $p < 0.01$, $p < 0.01$) in supplementary Table 2. On the other hand, the number of patients and the quality scores did not impact the pooled results, with $p > 0.05$ ($p = 0.95$ and $p = 0.27$) (supplementary Table 2).

For a comparison of the magnetic resonance (MR) scanner generations, we added magnetic field strength (1.5-T vs 3.0-T scanner) as a covariate to the bivariate model. For the 1.5-T scanner, the pooled sensitivity and specificity were 89% (95% CI, 85–92%) and 89% (95% CI, 84–93%) (supplementary Fig. 2); for the 3.0-T scanner, the pooled sensitivity and specificity were 77% (95% CI, 56–90%) and 97% (95% CI, 94–98%) (supplementary Fig. 3). The positive LR and negative LR were 8.40 (95% CI, 5.55–12.72) and 0.12 (95% CI, 0.08–0.18) for the 1.5-T scanner (supplementary Fig. 2). The 1.5-T scanner could increase the post-test probability of IPH to > 80% in patients with a pre-test probability of IPH > 33% and decrease the post-test probability of IPH to < 20% in patients with a pre-test probability of IPH < 67% (supplementary Fig. 4). The pooled results indicated that the sensitivity decreased from the 1.5- to 3.0-T scanner, while the specificity followed the opposite trend. For the 3.0-T scanner, the positive LR increased to 23.05 (95% CI, 11.70–45.43), and the negative LR also grew to 0.25 (95% CI, 0.12–0.50; supplementary Fig. 3). Importantly, the 3.0-T scanner, with excellent specificity and positive LR, could increase the post-test probability of IPH to > 80% in patients with a pre-test probability > 13%. It could also decrease the post-test probability of IPH to < 20% in patients with a pre-test probability < 51% (Fig. 4).

Though we found some factors that influenced the pooled results—such as different sequences of MRI, age, and gender—we cannot conduct a subgroup analysis for the limited number of references of different data.

We performed the sensitivity analysis to research the influence of each independent study. It indicated that no study influenced the pooled sensitivity and specificity results more than 0.03 (supplementary Fig. 4).

Discussion

In this meta-analysis, we analyzed 696 patients from 20 studies to investigate the accuracy of MRI in diagnosing IPH and to provide a clinical guide for MRI applications. The results demonstrated a good sensitivity of 87% as well as an excellent specificity of 92%. Further analysis revealed that MRI had favorable positive and negative predictive value profiles over a wide range of pre-test probabilities for IPH, which implies that MRI can be applied as an effective test to confirm or exclude carotid atherosclerotic IPH.

Plaque-derived stroke, because of its high rate of mortality, requires a precise diagnosis of plaque characteristics for risk stratification and medical treatment. IPH is a major mechanism for the progression of vulnerable atherosclerotic plaque and IPH plays an important role in the pathogenesis of clinical events [41, 45]. Early recognition of IPH and vulnerable plaque may be important clinical value in optimizing treatment to decrease the future sequelae [46].

Due to the degradation of hemorrhage into methemoglobin, which impacts magnetic susceptibility, MR is a relevant tool for detecting IPH in vivo [47]. Many studies have demonstrated the importance of MRI-detected IPH in predicting cerebrovascular events, which implies that IPH diagnosed by MRI is associated with vulnerable plaque [48–50]. These studies were based on the idea that the high signal on T1-weighed image was related to pathological IPH. However, there was variation in the accuracy of MRI for depicting IPH form one study to another in relevant diagnostic studies, with sensitivities of 86% to 96% and specificities of 75% to 82% [33, 40, 41]. Although several studies reported that MRI could detect IPH with excellent reliability and accuracy [20, 28, 44], the number of enrolled patients (from 11 to 135) and the use of single-center study designs limited the robustness of the conclusions. Tradeoffs between sensitivity, specificity, and disease probability must be simultaneously evaluated for judging which strategy could maximize clinical utility. So, besides the sensitivity and specificity, the disease probability should also be taken into account, which is important for diagnostic decisions and expected clinical utility [51].

In addition to good sensitivity and high specificity for diagnosing carotid IPH, this meta-analysis showed a high accuracy of MRI (AUROC = 0.95). To determine the implications of our results for clinical decision-making, we calculated the post-test probabilities of MRI for populations with different pre-test probabilities of IPH (Fig. 4). The results indicated a high positive predictive value across a broad spectrum of pre-test probabilities. MRI also demonstrated a good negative

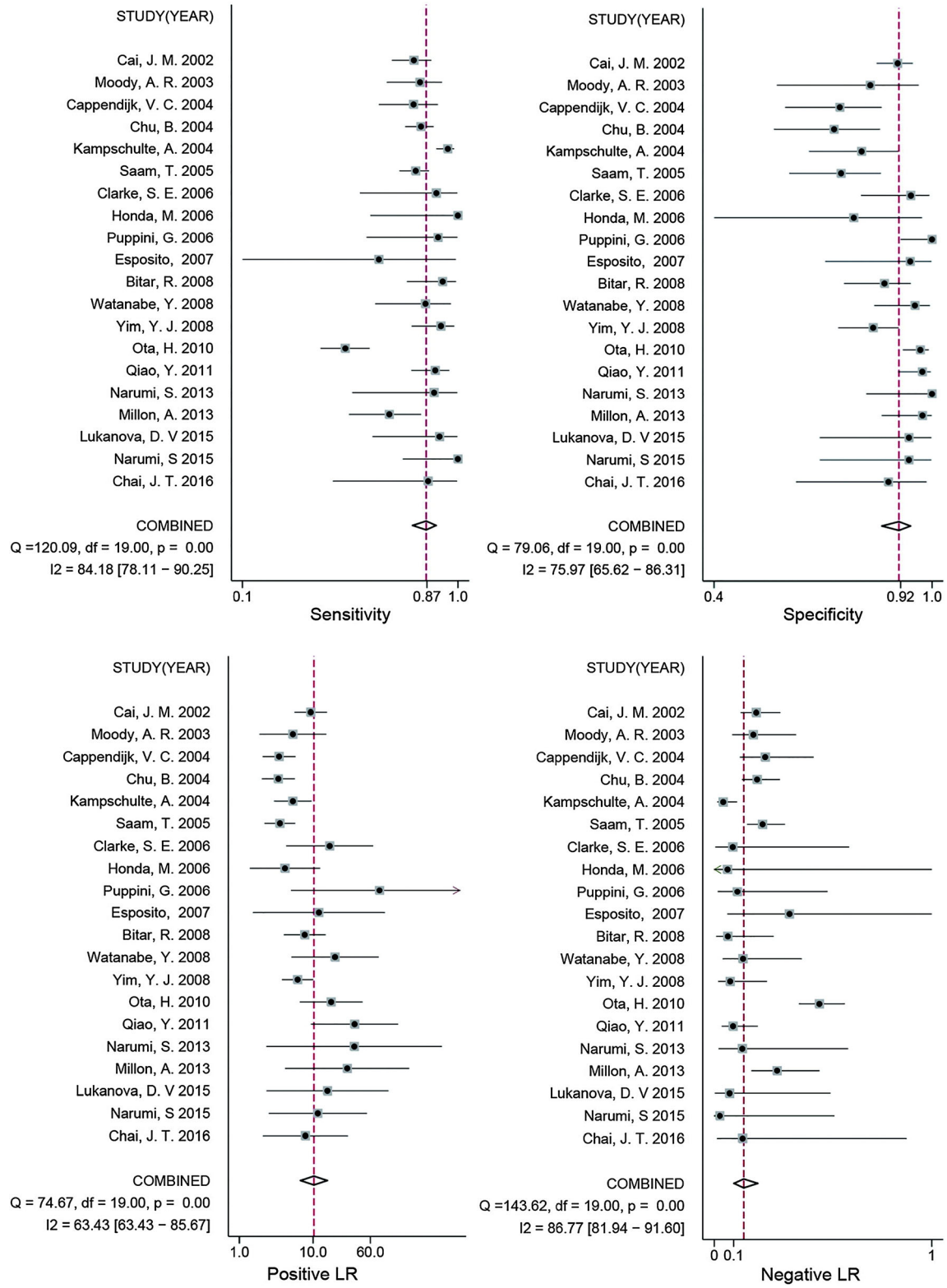

Fig. 2 Forest plots illustrating detailed sensitivity, specificity, positive LR, and negative LR. The pooled sensitivity was good and specificity was excellent with results of 87% (95% CI, 81–91%) and 92% (95% CI, 87–95%), respectively. The positive and negative LRs were 10.27 (95% CI, 6.76–15.59) and 0.15 (95% CI, 0.10–0.21), respectively

diagnostic capability. MRI-detected IPH represents an imaging biomarker for vulnerable plaque and thus improves the establishment of a clinical prognosis as well as the determination of personalized treatment.

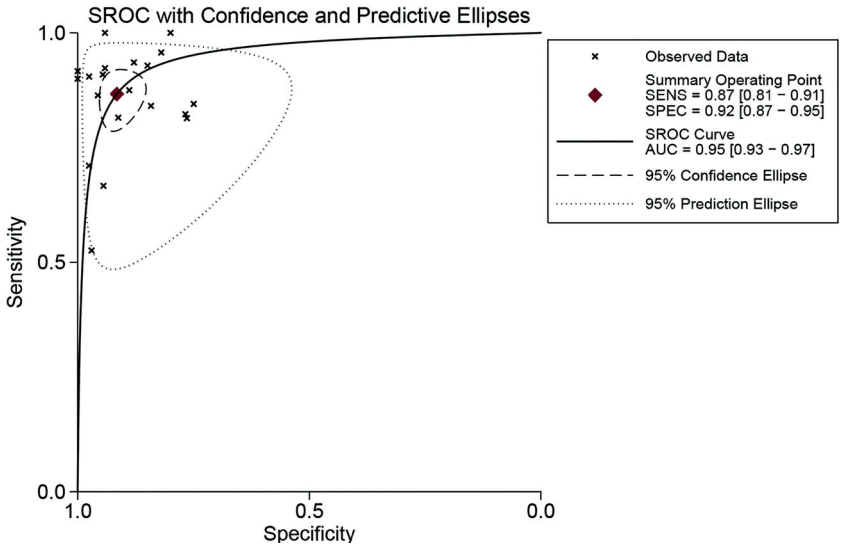

Fig. 3 Summary receiver-operating characteristic (SROC) curve of MRI. We calculated estimates of the diagnostic performance of MRI obtained from the bivariate random-effects meta-analysis. The area under the curve was 0.95 (95% CI, 0.93–0.97), which indicated a high accuracy of MRI in diagnosing IPH

The present analysis demonstrates that MRI could identify not only 920 true-negative and 837 true-positive cases but also 167 false-negative and 99 false-positive cases. The false results may derive from the inherent shortcomings of MRI. Although MRI has high accuracy and systematic criteria for diagnosing a cerebral hemorrhage, it is difficult to directly extrapolate the hemorrhage criteria from cerebral events to IPH. First, IPH may insinuate itself into preexisting necrotic cores or into spaces between calcifications and matrices, which results in a wide range of MR signal intensity [41]. Another potential reason is the hypointensity of the "old" IPH [41]. Most studies only select those areas with hyperintense T1-weighted images for analysis. Although hemorrhagic lesions are identified solely on the basis of high signal intensity, the old IPH with hypointensity in all contrast weightings is generally classified as calcification by mistake [41]. Furthermore, the lipid-rich necrotic core, the intact degenerating red cells, and the increase interstitial fluid

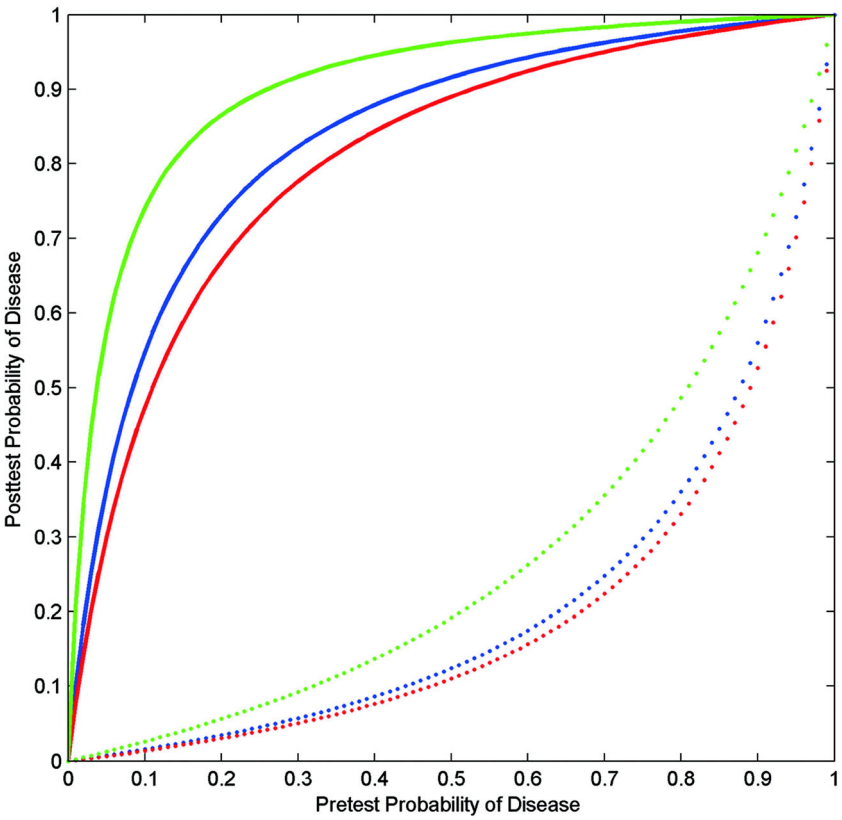

Fig. 4 Bayesian plots of pre- and post-test probabilities. The plot illustrates the post-test probability after negative or positive findings on MRI for populations with different prevalence rates (pre-test probabilities) of IPH. As a whole, MRI could increase the post-test probability of IPH to > 80% in patients with pre-test probability > 27% (blue solid line) and could decrease post-test probability of IPH to < 20% in patients with a pre-test probability < 64% (blue dotted line). 3.0-T scanner could increase post-test probability to > 80% in patients with a pre-test probability > 13% (green solid line), whose positive predictive value was better than that of 1.5-T scanner (red solid line). However, the negative predictive value of 3.0-T scanner (green dotted line) was worse than that of 1.5-T scanner (red dotted line)

associated with inflammation may increase hyperintense signal and lead to false positives [31, 41]. On the TOF sequence, the signal may also be affected by the high signal intensity of flowing blood within an ulcer and the motion artifacts [30].

Because of anticipated heterogeneity, we used a random-effects model to consider the heterogeneity, further explored the heterogeneity by adding covariates to the meta-regression analysis, and performed subgroup analyses. The results indicated that the significant predictors were magnetic field strength, different MRI sequences, age, and gender. Although heterogeneity was present—a common situation in diagnostic meta-analyses—we believe that the heterogeneity was more statistical than clinical. The pooled results are particularly relevant for harmonizing the diagnostic standards for future studies and clinical decisions.

An intergenerational comparison shows that the specificity of the 3.0-T scanner (97%) is significantly higher than that of the 1.5-T scanner (89%). Moreover, the 3.0-T scanner may have an excellent positive predictive value profile across a wide range of pre-test probabilities for IPH (> 13%). On the other hand, the 1.5-T scanner shows a worse positive predictive ability and can identify IPH in patients with a pre-test probability > 33%. The improved performance of the 3.0-T scanner can be attributed to the reduced $T2^*$ and T2 of the fibrous tissue in higher field strengths, which leads to better discrimination between IPH and collagen-rich structure [31]. Although the specificity increases with higher field strengths, the sensitivity follows the opposite trend, with a better pooled value in the 1.5-T group (89% vs 77%). The potential reason may be that the 3.0-T scanner can increase the susceptibility of calcification and paramagnetic ferric iron in IPH. The more pronounced susceptibility effect may lead to cancelation of the signal enhancement with T1-weighted sequences, which may alter hemorrhage quantification and/or detection and results in a false negative [31]. Although both the 1.5-T and 3.0-T MRI have high specificity and sensitivity for diagnosing IPH, we recommend the 3.0-T scanner, as it detects more positive IPH.

MR sequence differences may also explain inconsistencies. IPH imaging is mainly dependent on the T1 shortening effects of methemoglobin [52], evaluated for instance on 2-D T1 fast-spin echo sequence or 3-D T1 gradient-echo sequence or magnetization-prepared RAGE MRI. As magnetization-prepared RAGE imaging suppresses the signals from components with a relatively long T1—such as fibrous tissue and the lipid-rich necrotic core—it facilitates the image interpretation through the hypointense appearance of the background and may improve the signal-to-noise ratios and contrast-to-noise ratios [31]. Moreover, the 3-D technique is inherently related to higher signal-to-noise ratios and contrast-to-noise ratios, better depicting the carotid vessel wall and the carotid IPH [20, 31, 34]. Although a single T1WI could diagnose the methemoglobin in IPH accurately in practice, multicontrast sequences (TOF, T1W, PDW, and T2W) are generally applied to distinguish the stage of IPH [39, 41]. In short, fresh IPH shows an isointense signal on T2W/PDW images and a hyperintense signal on T1W and TOF images, while recent but not fresh hemorrhage appears as a hyperintense signal on all four combined sequences [41]. In addition, the use of TOF images improves the ability to distinguish necrotic cores and IPH, which may be more challenging with T1W images [53]. Although we cannot perform the relevant subgroup analysis, we recommend a multiparameter MRI assessment.

Importantly, the present meta-analysis indicates that gender and age may influence the diagnostic performance. Artery calcification is related to gender and age [54]. Because plaque calcifications are sensitive to the magnetic-susceptibility effect, heavy carotid plaque calcification in males and elder people can significantly affect the diagnostic accuracy of MRI [30, 41].

Limitations

First, we could not obtain the detailed data that could link IPH to its exact clinical symptoms so that an index of clinical importance could be generated and considered for a pooled analysis. The answer to the question "What should be used as the reference standard?" may vary according to whether the purpose is to detect IPH—in which case, the histology would be the gold standard—or to stratify risk, in which case, the gold standard is long-term follow-ups. Two meta-analyses have addressed the predictive power of MRI-detected IPH for clinical events, which showed different hazard ratios [48, 55]. This difference could be in part related due to different field strengths. Saam et al reported a hazard ratio of 5.69 by analyzing eight studies based on 1.5-T scanners [48], while Gupta et al concluded a hazard ratio of 4.59 from six 1.5-T and one 3.0-T scanner studies [55]. It should be noted that, by far, the majority of studies on IPH have been performed in a sample of selected patient. Population-based evidence for an association of IPH with the risk of a first stroke remains limited. In the future, the results of MRI-detected IPH from population-based cohorts would significantly contribute to determining the predictive clinical value of IPH for first strokes. Second, all these studies had single-center designs and low sample sizes. This raises concerns about the generalizability of our results for actual clinical practice settings, where variation in operator performance and data-acquisition protocols may produce less-remarkable results than those presented in the pooled analysis. A sensitivity analysis was performed to test if the pooled results were sensitive to the restrictions on the data. After the exclusion of subsequent studies published from a single academic center with a low sample size, the results showed no change in sensitivity or specificity. Third, the amount of unstable plaques in asymptomatic patients was unclear due to a lack of relevant information in many articles.

Finally, we cannot evaluate the impact of smoking, hypercholesterolemia, hypertension, and diabetes on the diagnostic accuracy due to the limited data.

Conclusion

Our analysis suggests that non-invasive MRI has an excellent specificity and a good sensitivity for diagnosing IPH. MRI is a tool for confirming or ruling out carotid atherosclerotic IPH.

Funding This study has received funding by grants from the National Key R&D Program of China (2016YFC1300300).

Compliance with ethical standards

Guarantor The scientific guarantor of this publication is Gang Sun.

Conflict of interest The authors of this manuscript declare no relationships with any companies whose products or services may be related to the subject matter of the article.

Statistics and biometry The author Min Li has significant statistical expertise.

Informed consent Written informed consent was not required for this study because all analyses were based on previously published studies; thus, no patient consent is required.

Ethical approval Institutional Review Board approval was not required because all analyses were based on previously published studies; thus, no ethical approval is required.

Methodology
- prospective
- diagnostic study
- multicenter study

References

1. Howard DP, van Lammeren GW, Rothwell PM et al (2015) Symptomatic carotid atherosclerotic disease: correlations between plaque composition and ipsilateral stroke risk. Stroke 46:182–189
2. Park JS, Kwak HS, Lee JM, Koh EJ, Chung GH, Hwang SB (2015) Association of carotid intraplaque hemorrhage and territorial acute infarction in patients with acute neurological symptoms using carotid magnetization-prepared rapid acquisition with gradient-echo. J Korean Neurosurg Soc 57:94–99
3. Halliday A, Harrison M, Hayter E et al (2010) 10-year stroke prevention after successful carotid endarterectomy for asymptomatic stenosis (ACST-1): a multicentre randomised trial. Lancet 376: 1074–1084
4. Barnett HJM, Taylor DW, Haynes RB et al (1991) Beneficial effect of carotid endarterectomy in symptomatic patients with high-grade carotid stenosis. N Engl J Med 325:445–453
5. Brinjikji W, Huston J 3rd, Rabinstein AA, Kim GM, Lerman A, Lanzino G (2016) Contemporary carotid imaging: from degree of stenosis to plaque vulnerability. J Neurosurg 124:27–42
6. Freilinger TM, Schindler A, Schmidt C et al (2012) Prevalence of nonstenosing, complicated atherosclerotic plaques in cryptogenic stroke. JACC Cardiovasc Imaging 5:397–405
7. Kolodgie FD, Yahagi K, Mori H et al (2017) High-risk carotid plaque: lessons learned from histopathology. Semin Vasc Surg 30: 31–43
8. Zhao Q, Zhao X, Cai Z, Li F, Yuan C, Cai J (2011) Correlation of coronary plaque phenotype and carotid atherosclerotic plaque composition. Am J Med Sci 342:480–485
9. McNally JS, McLaughlin MS, Hinckley PJ et al (2015) Intraluminal thrombus, intraplaque hemorrhage, plaque thickness, and current smoking optimally predict carotid stroke. Stroke 46: 84–90
10. Fisher M, Paganini-Hill A, Martin A et al (2005) Carotid plaque pathology: thrombosis, ulceration, and stroke pathogenesis. Stroke 36:253–257
11. Stary HC (2000) Natural history and histological classification of atherosclerotic lesions: an update. Arterioscler Thromb Vasc Biol 20:1177–1178
12. Ramnarine KV, Garrard JW, Kanber B, Nduwayo S, Hartshorne TC, Robinson TG (2014) Shear wave elastography imaging of carotid plaques: feasible, reproducible and of clinical potential. Cardiovasc Ultrasound 12:49
13. Kanber B, Hartshorne TC, Horsfield MA, Naylor AR, Robinson TG, Ramnarine KV (2015) A novel ultrasound-based carotid plaque risk index associated with the presence of cerebrovascular symptoms. Ultraschall Med 36:480–486
14. Kwee RM, van Oostenbrugge RJ, Hofstra L et al (2008) Identifying vulnerable carotid plaques by noninvasive imaging. Neurology 70: 2401–2409
15. Arai D, Yamaguchi S, Murakami M et al (2011) Characteristics of carotid plaque findings on ultrasonography and black blood magnetic resonance imaging in comparison with pathological findings. Acta Neurochir Suppl 112:15–19
16. Shimada Y, Oikawa K, Fujiwara S et al (2017) Comparison of three-dimensional T1-weighted magnetic resonance and contrast-enhanced ultrasound plaque images for severe stenosis of the cervical carotid artery. J Stroke Cerebrovasc Dis 26:1916–1922
17. Rafailidis V, Chryssogonidis I, Xerras C et al (2018) A comparative study of color Doppler imaging and contrast-enhanced ultrasound for the detection of ulceration in patients with carotid atherosclerotic disease. Eur Radiol. https://doi.org/10.1007/s00330-018-5773-8
18. Yao B, Yang L, Wang G et al (2016) Diffusion measurement of intraplaque hemorrhage and intramural hematoma using diffusion weighted MRI at 3T in cervical artery. Eur Radiol 26:3737–3743
19. Chai JT, Biasiolli L, Li L et al (2016) Quantification of lipid-rich core in carotid atherosclerosis using magnetic resonance T2 mapping: relation to clinical presentation. JACC Cardiovasc Imaging 10:747–756
20. Narumi S, Sasaki M, Natori T et al (2015) Carotid plaque characterization using 3D T1-weighted MR imaging with histopathologic validation: a comparison with 2D technique. AJNR Am J Neuroradiol 36:751–756
21. Whiting P, Rutjes AW, Reitsma JB, Bossuyt PM, Kleijnen J (2003) The development of QUADAS: a tool for the quality assessment of studies of diagnostic accuracy included in systematic reviews. BMC Med Res Methodol 3:25
22. Deeks JJ, Macaskill P, Irwig L (2005) The performance of tests of publication bias and other sample size effects in systematic reviews of diagnostic test accuracy was assessed. J Clin Epidemiol 58:882–893
23. Reitsma JB, Glas AS, Rutjes AW, Scholten RJ, Bossuyt PM, Zwinderman AH (2005) Bivariate analysis of sensitivity and

specificity produces informative summary measures in diagnostic reviews. J Clin Epidemiol 58:982–990
24. Chu H, Cole SR (2006) Bivariate meta-analysis of sensitivity and specificity with sparse data: a generalized linear mixed model approach. J Clin Epidemiol 59:1331–1332 author reply 1332-1333
25. Higgins JP, Thompson SG, Deeks JJ, Altman DG (2003) Measuring inconsistency in meta-analyses. BMJ 327:557–560
26. Jaeschke R, Guyatt GH, Sackett DL (1994) Users' guides to the medical literature. III. How to use an article about a diagnostic test. B. What are the results and will they help me in caring for my patients? The Evidence-Based Medicine Working Group. JAMA 271:703–707
27. Lukanova DV, Nikolov NK, Genova KZ, Stankev MD, Georgieva EV (2015) The accuracy of noninvasive imaging techniques in diagnosis of carotid plaque morphology. Open Access Maced J Med Sci 3:224–230
28. Millon A, Mathevet JL, Boussel L et al (2013) High-resolution magnetic resonance imaging of carotid atherosclerosis identifies vulnerable carotid plaques. J Vasc Surg 57:1046–1051.e2
29. Narumi S, Sasaki M, Ohba H et al (2013) Prediction of carotid plaque characteristics using non-gated MR imaging: correlation with endarterectomy specimens. AJNR Am J Neuroradiol 34: 191–197
30. Qiao Y, Etesami M, Malhotra S et al (2011) Identification of intraplaque hemorrhage on MR angiography images: a comparison of contrast-enhanced mask and time-of-flight techniques. AJNR Am J Neuroradiol 32:454–459
31. Ota H, Yarnykh VL, Ferguson MS et al (2010) Carotid intraplaque hemorrhage imaging at 3.0-T MR imaging: comparison of the diagnostic performance of three T1-weighted sequences. Radiology 254:551–563
32. Yim YJ, Choe YH, Ko Y et al (2008) High signal intensity halo around the carotid artery on maximum intensity projection images of time-of-flight MR angiography: a new sign for intraplaque hemorrhage. J Magn Reson Imaging 27:1341–1346
33. Watanabe Y, Nagayama M, Suga T et al (2008) Characterization of atherosclerotic plaque of carotid arteries with histopathological correlation: vascular wall MR imaging vs. color Doppler ultrasonography (US). J Magn Reson Imaging 28:478–485
34. Bitar R, Moody AR, Leung G et al (2008) In vivo 3D high-spatial-resolution MR imaging of intraplaque hemorrhage. Radiology 249: 259–267
35. Esposito L, Sievers M, Sander D et al (2007) Detection of unstable carotid artery stenosis using MRI. J Neurol 254:1714–1722
36. Puppini G, Furlan F, Cirota N et al (2006) Characterisation of carotid atherosclerotic plaque: comparison between magnetic resonance imaging and histology. Radiol Med 111:921–930
37. Honda M, Kitagawa N, Tsutsumi K, Nagata I, Morikawa M, Hayashi T (2006) High-resolution magnetic resonance imaging for detection of carotid plaques. Neurosurgery 58:338–346 discussion 338-346
38. Clarke SE, Beletsky V, Hammond RR, Hegele RA, Rutt BK (2006) Validation of automatically classified magnetic resonance images for carotid plaque compositional analysis. Stroke 37:93–97
39. Saam T, Ferguson MS, Yarnykh VL et al (2005) Quantitative evaluation of carotid plaque composition by in vivo MRI. Arterioscler Thromb Vasc Biol 25:234–239
40. Kampschulte A, Ferguson MS, Kerwin WS et al (2004) Differentiation of intraplaque versus juxtaluminal hemorrhage/thrombus in advanced human carotid atherosclerotic lesions by in vivo magnetic resonance imaging. Circulation 110:3239–3244
41. Chu B, Kampschulte A, Ferguson MS et al (2004) Hemorrhage in the atherosclerotic carotid plaque: a high-resolution MRI study. Stroke 35:1079–1084
42. Cappendijk VC, Cleutjens KB, Heeneman S et al (2004) In vivo detection of hemorrhage in human atherosclerotic plaques with magnetic resonance imaging. J Magn Reson Imaging 20:105–110
43. Moody AR, Murphy RE, Morgan PS et al (2003) Characterization of complicated carotid plaque with magnetic resonance direct thrombus imaging in patients with cerebral ischemia. Circulation 107:3047–3052
44. Cai JM, Hatsukami TS, Ferguson MS, Small R, Polissar NL, Yuan C (2002) Classification of human carotid atherosclerotic lesions with in vivo multicontrast magnetic resonance imaging. Circulation 106:1368–1373
45. Wang X, Sun J, Zhao X et al (2017) Ipsilateral plaques display higher T1 signals than contralateral plaques in recently symptomatic patients with bilateral carotid intraplaque hemorrhage. Atherosclerosis 257:78–85
46. Sun J, Underhill HR, Hippe DS, Xue Y, Yuan C, Hatsukami TS (2012) Sustained acceleration in carotid atherosclerotic plaque progression with intraplaque hemorrhage: a long-term time course study. JACC Cardiovasc Imaging 5:798–804
47. Raman SV, Winner MW 3rd, Tran T et al (2008) In vivo atherosclerotic plaque characterization using magnetic susceptibility distinguishes symptom-producing plaques. JACC Cardiovasc Imaging 1:49–57
48. Saam T, Hetterich H, Hoffmann V et al (2013) Meta-analysis and systematic review of the predictive value of carotid plaque hemorrhage on cerebrovascular events by magnetic resonance imaging. J Am Coll Cardiol 62:1081–1091
49. Li D, Zhao H, Chen X et al (2018) Identification of intraplaque haemorrhage in carotid artery by simultaneous non-contrast angiography and intraPlaque haemorrhage (SNAP) imaging: a magnetic resonance vessel wall imaging study. Eur Radiol 28:1681–1686
50. Oei ML, Ozgun M, Seifarth H et al (2010) T1-weighted MRI for the detection of coronary artery plaque haemorrhage. Eur Radiol 20: 2817–2823
51. Boyko EJ (1994) Ruling out or ruling in disease with the most sensitive or specific diagnostic test: short cut or wrong turn? Med Decis Making 14:175–179
52. Yamada N, Higashi M, Otsubo R et al (2007) Association between signal hyperintensity on T1-weighted MR imaging of carotid plaques and ipsilateral ischemic events. AJNR Am J Neuroradiol 28:287–292
53. Yuan C, Mitsumori LM, Ferguson MS et al (2001) In vivo accuracy of multispectral magnetic resonance imaging for identifying lipid-rich necrotic cores and intraplaque hemorrhage in advanced human carotid plaques. Circulation 104:2051–2056
54. Sun J, Zhao XQ, Balu N et al (2017) Carotid plaque lipid content and fibrous cap status predict systemic CV outcomes: the MRI substudy in AIM-HIGH. JACC Cardiovasc Imaging 10:241–249
55. Gupta A, Baradaran H, Schweitzer AD et al (2013) Carotid plaque MRI and stroke risk: a systematic review and meta-analysis. Stroke 44:3071–3077